# Model Reduction of Power System Dynamics using a Constrained Convex-optimization Method

Sanjana Vijayshankar, Maziar S. Hemati, Andrew Lamperski, Sairaj Dhople

***Abstract*— This paper discusses methods for model reduction of power system dynamics. Dynamical models for realistic power-systems can very easily contain several thousands of states. The dimensionality increases further when considering the dynamics of distributed energy resources; these systems are typically smaller in power rating, so many more are installed at the grid edge to scale capacity. Computationally efficient models that capture the dominant modes of the system are important for all aspects of power-system operation, control, and analysis. In this paper, we analyze two data-driven methods for model reduction of power systems: i) proper orthogonal decomposition, which is based on singular value decomposition, and ii) a constrained convex-optimization framework with stability guarantees. Advantages and disadvantages of both of these methods are discussed. Exhaustive numerical simulations for a low-inertia system with mixed synchronous generator and wind energy conversion system resources are provided to verify the accuracy of the model-reduction methods.**

## I. Introduction

The dimension of state-space models that describe power-system dynamics can easily contain a few thousand states. This imposes a considerable computational burden on applications such as small signal stability analysis, dynamic simulation, sensitivity analysis, and control design. With the addition of renewable energy resources to the grid like wind and solar, the state dimension of the system can grow by another order of magnitude. The reason being that typical ratings of these resources is far below that of conventional fossil-driven generation; consequently, to scale capacity, many such units would need to be installed. Furthermore, with the introduction of such resources, the dynamical models that capture the electromechanical and/or electromagnetic behavior of the system may not be perfectly known due to parametric uncertainty or they may not be homogeneous and structured: attributes that have long been leveraged for a variety of tasks spanning modeling, analysis, and control design for bulk power systems dominated by synchronous generators.

The challenges highlighted above imply that model-reduction methods are critical to facilitate operations and control in power systems. Broadly, the choice of model-reduction method primarily depends on the properties of a given system that are to be retained in the reduced-order model. Of the scores of analytical, numerical, and data-driven approaches that have been proposed in the literature, two types of methods are particularly relevant in the context of this work: those motivated by obtaining a balanced (i.e., it is as controllable as it is observable) realization of the system; and data-driven methods grounded in singular value decomposition (SVD) of time-series data collected from the originating system. Balanced model reduction [1], [2] innately offers stability guarantees on the reduced order model whereas SVD-based data-driven methods [3] are prone to instability. Model reduction has been a widely studied topic in the context of power-system dynamics [4], [5] given that most tasks related to small signal stability analysis and control design would be intractable (analytically and computationally) for the originating nonlinear full-order-system differential algebraic equation models. Most methods for model reduction focus on obtaining a linearized representation of the underlying dynamics, which, in many cases provides accurate descriptions of pertinent electromagnetic and electromechanical behavior [3], [6]. Specific methods of note include: i) *Coherency* [7], [8], which is an approach by which generators that belonging to the same coherent group are aggregated, thereby reducing the dimension of the system dynamical model; and ii) *Singular perturbation analysis* [9], where timescales are explicitly partitioned and dynamics at a given time-scale are retained in the reduced-order model. Data-driven and optimization-based methods, however, have received limited attention. A few notable contributions in this domain include [10], [11].

This paper develops two data-driven techniques for model reduction. First, an SVD based method called Proper Orthogonal Decomposition (POD) is applied to project linearized power-system dynamics to a lower dimensional subspace. POD has no analytical guarantees for the stability of the reduced-order system. As a mitigatory solution to this particular concern, the second method we put forth involves an optimization framework for model reduction that preserves stability of the originating full-order model. The approach is an extension of a convex-optimization method developed by Lacy and Bernstein [12] for system identification. Our approach builds off this method, and leverages it for model reduction by appending rank constraints in the involved optimization problem to yield a low-rank solution. Furthermore, we also put forth a linear relaxation of the problem to ensure computational efficiency. From an application standpoint, we want to emphasize that the data-driven foundation of the proposed method is perfectly aligned with the task of obtaining reduced-order models where the underlying

Sanjana Vijayshankar, Andrew Lamperski, and Sairaj Dhople are with the Department of Electrical and Computer Engineering, University of Minnesota, Minneapolis, MN 55455. E-mails: {vijay092, alampers, sdhople}@umn.edu. Maziar S. Hemati is with the Department of Aerospace Engineering and Mechanics, University of Minnesota, Minneapolis, MN 55455. E-mail: mhemati@umn.edu. This work is supported in part by the National Science Foundation through award 1453921.

dynamics are due to heterogeneous energy-conversion interfaces or model parameters may not be perfectly known. This induces significant modeling complexity and renders analytical approaches intractable. With this general feature in mind, we provide simulation results for a setting that might be representative of a future low-inertia power system: a network composed of synchronous generators and power-electronics based wind energy conversion systems (WECS) with inertial and droop control.

The remainder of this paper is organized as follows. In Section II, we describe the dynamical models of the system. Next, we discuss the two methods for model reduction in Section III. We present results for each one of these in Section IV. Finally, we conclude the paper in Section V.

## II. Models for Synchronous Generator, WECS, and Network

In this section, we describe the differential-algebraic equation (DAE) models that capture the electromechanical dynamics of synchronous generators and wind turbines in a power network. We provide an abridged discussion (leaving out precise details with regard to state variables, algebraic variables, filter parameters, and controller gains) for the dynamical models. For specific details, we point out that the synchronous machine model is adopted from [13], while the WECS model is based on our previous work [14].

### A. Synchronous Generator Model

The synchronous generators are modeled with a two-axis model and governor dynamics are ignored. The terminal voltage is governed by a voltage regulator and associated exciter circuitry. An IEEE Type-I exciter (which utilizes a first-order lead-lag compensator) is assumed. The DAE model governing the synchronous generator dynamics is of the general form:

$$\dot{x}_{\mathrm{m}} = f_{\mathrm{m}}(x_{\mathrm{m}}, z_{\mathrm{m}}, u_{\mathrm{m}}), \tag{1}$$

$$0 = g_{\mathrm{m}}(x_{\mathrm{m}}, z_{\mathrm{m}}, u_{\mathrm{m}}), \tag{2}$$

where the dynamic states, $x_{\mathrm{m}}$, algebraic variables, $z_{\mathrm{m}}$, and inputs $u_{\mathrm{m}}$ of the machine are:

$$x_{\mathrm{m}} = [E'_{\mathrm{d}}, E'_{\mathrm{q}}, \delta_{\mathrm{g}}, \omega, E_{\mathrm{fd}}, V_{\mathrm{R}}, R_{\mathrm{F}}]^{\mathrm{T}}, \tag{3}$$

$$z_{\mathrm{m}} = [I_{\mathrm{d}}, I_{\mathrm{q}}]^{\mathrm{T}},\ u_{\mathrm{m}} = [V_{\mathrm{ref}}, T_{\mathrm{m}}]^{\mathrm{T}}. \tag{4}$$

A brief overview of the dynamic and algebraic states is as follows: $E'_{\mathrm{d}}$ and $E'_{\mathrm{q}}$ are the direct and quadrature-axis transient internal voltages; $\delta_{\mathrm{g}}$ and $\omega$ are the machine angle and frequency, respectively; $E_{\mathrm{fd}}$ is the field voltage; $V_{\mathrm{R}}$ and $R_{\mathrm{F}}$ are the voltage regulator state and the rate feedback state of the voltage regulator, respectively. The machine terminal currents, $I_{\mathrm{d}}$ and $I_{\mathrm{q}}$, serve as the algebraic states. Inputs include the mechanical torque $T_{\mathrm{m}}$ and the voltage reference for the exciter circuitry, $V_{\mathrm{ref}}$. Closed-form expressions for the functions $f_{\mathrm{m}} : \mathbb{R}^7 \times \mathbb{R}^2 \times \mathbb{R}^2 \to \mathbb{R}^7$ and $g_{\mathrm{m}} : \mathbb{R}^7 \times \mathbb{R}^2 \times \mathbb{R}^2 \to \mathbb{R}^2$ are available in [13], and not explicitly spelled out here due to space constraints.

### B. Wind Energy Conversion System (WECS) Model

The WECS is assumed to be composed of Type-3 wind turbines. Type-3 turbine dynamical models are composed of the following sub-systems: aerodynamics, doubly fed induction generator (DFIG), rotor-side converter , grid-side converter, DC-link capacitor, and other filters. The turbine aerodynamic model captures the dynamics of the generator speed and turbine rotor speed. Stator currents and rotor transient voltages are the states of the DFIG. The rotor side converter includes outer-loop reactive-power and electromagnetic-torque controllers, and inner-loop current controllers. The grid-side converter consists of a full-bridge inverter, and the corresponding control architecture is composed of a phase-locked loop (PLL), an outer-loop power controller, and an inner-loop current controller. In all, each turbine has 27 state variables [14].

In our previous work [14], we have established parametric scalings with which one can obtain an aggregated reduced-order model with the same dimension and structure as any wind turbine in a WECS composed of $N$ turbines. That is, a wind farm dynamical model can be derived with the same model order as that of an individual turbine (which is 27 in this case). We provide a brief overview of what such an aggregate model involves. Inductances and resistances in output filters are scaled by a factor of $N^{-1}$, while the DC-link capacitance is scaled by $N$ given the parallel interconnection. Pertinent controller gains for current controllers are also appropriately scaled, while controller gains for the PLL and power-side controllers are unchanged. These scalings make intuitive sense given the parallel interconnection. In effect, the state-space model for a WECS composed of $N$ Type-3 turbines can be expressed in the form:

$$\dot{x}_{\mathrm{w}} = f_{\mathrm{w}}(x_{\mathrm{w}}, u_{\mathrm{w}}), \tag{5}$$

where, we refrain from explicitly listing and describing all 27 states to preserve brevity of discussion, and the inputs are as follows:

$$u_{\mathrm{w}} = [Nq^*, v_{\mathrm{g}}^{\mathrm{a}}, v_{\mathrm{g}}^{\mathrm{b}}, v_{\mathrm{g}}^{\mathrm{c}}, v_{\mathrm{w}}]^{\mathrm{T}}. \tag{6}$$

The inputs to the model are the wind speed, $v_{\mathrm{w}}$, reactive power references for the turbines, $q^\star$, and grid voltages, $v_{\mathrm{g}}^{\mathrm{a}}, v_{\mathrm{g}}^{\mathrm{b}}, v_{\mathrm{g}}^{\mathrm{c}}$. A detailed description of all entries of the nonlinear function $f_{\mathrm{w}} : \mathbb{R}^{27} \times \mathbb{R}^5 \to \mathbb{R}^{27}$ capturing all aerodynamic, electromechanical, controller, and filter dynamics is provided in [14].

### C. Power Network Model

Interactions of the different energy-conversion interfaces in the power network are captured by Kirchoff's laws. These algebraic equations can be significantly simplified by eliminating nodes in the network with zero-power injections through a process called Kron reduction. The algebraic equations that describe the interconnection of the wind farm and the synchronous generators through the electrical network can be subsequently compactly written as:

$$0 = g_{\mathrm{n}}(x_{\mathrm{w}}, u_{\mathrm{w}}, z_{\mathrm{m}}). \tag{7}$$

It so emerges for a network with impedance-based loads, that the function $g_{\rm n}$ is such that the algebraic variables can be explicitly expressed as functions of dynamic states. In short, this means that the complete model can be expressed only with dynamic equations and it can be subsequently linearized around a suitable operating point.

A power network comprising $N_{\rm gen}$ synchronous generators and $N_{\rm WECS}$ WECS, each with say $N_{\rm tur}$ turbines would be described by a dynamical system model of order: $7 \times N_{\rm gen} + 27 \times N_{\rm WECS}$. (Notice that we do not have an additional factor of $N_{\rm tur}$ given that we employ an aggregated model for each WECS.) Evidently, modeling, analysis and control of such a system at scale ($N_{\rm gen} > 10$, $N_{\rm WECS} > 100$ for a realistically sized synchronous balancing area) would be infeasible and intractable with the original system models.

## III. Model Reduction Methods

Given the models for the synchronous generators, WECS and the power network in, (1), (5) and (7) respectively, we are interested in deriving a stability-preserving, discrete-time reduced-order model with $m$ inputs and $p$ outputs admitting the following representation:

$$\begin{aligned} x_{k+1} &= A_{\rm r} x_k + B_{\rm r} u_k, \\ y_k &= C_{\rm r} x_k + D_{\rm r} u_k. \end{aligned} \tag{8}$$

Above, $A_{\rm r} \in \mathbb{R}^{r\times r}$, $B_{\rm r} \in \mathbb{R}^{r\times m}$, $C_{\rm r} \in \mathbb{R}^{p\times r}$ and $D_{\rm r} \in \mathbb{R}^{p\times m}$. A similar representation expressed with matrices $A, B, C, D$ follows for the full-order stable discrete-time model that is obtained by suitably linearizing the originating dynamics. We next overview two methods to obtain the reduced-order model. In subsequent discussions, we will denote the dimension of the full-order model by $n$, and the dimension of the reduced-order model by $r$.

### A. Method I: POD-Galerkin Approach

Proper orthogonal decomposition (POD) [15], [16] is a method for obtaining a basis that optimally spans a given set of data. This basis may then be used for Galerkin projection which allows one to obtain a reduced-order representation [3]. Here we briefly discuss the method in the context of finite-dimensional systems.

First, we generate $l$ snapshots of system states for time indices $k, \ldots, k+l-1$ from the full-order model, and form an augmented data matrix:[1]

$$\Delta_x^{k:k+l-1} := \begin{bmatrix} x_k & x_{k+1} & \ldots & x_{k+l-1} \end{bmatrix} \in \mathbb{R}^{n\times l}. \tag{9}$$

Let us denote $\mathrm{rank}(\Delta_x^{k:k+l-1}) =: \rho_\Delta$. An economy-sized SVD of $\Delta_x^{k:k+l-1}$ is given by

$$\Delta_x^{k:k+l-1} = U\Sigma V^*, \tag{10}$$

where $(\cdot)^*$ denotes complex-conjugate transpose, the diagonal matrix $\Sigma \in \mathbb{R}^{\rho_\Delta \times \rho_\Delta}$ is invertible and includes all non-zero singular values, and $U^*U = V^*V = I_{n\times n}$. The columns of $U$ are called POD modes and the rows of $\Sigma V^*$ form the temporal amplitudes [3].

Following the approach in [15], the POD modes can be used to obtain a reduced-order model as below with the following Galerkin projection:

$$\begin{aligned} A_{\rm r} &= U_{\rm r}^* A U_{\rm r}, \quad B_{\rm r} = U_{\rm r}^* B, \\ C_{\rm r} &= C U_{\rm r}, \quad D_{\rm r} = D, \end{aligned} \tag{11}$$

where, recall that $A, B, C, D$ are system matrices for the full-order model, and $A_{\rm r}, B_{\rm r}, C_{\rm r}, D_{\rm r}$ are the corresponding reduced-order counterparts. Furthermore, $U_{\rm r}$ denotes the first $r \le \rho_\Delta$ columns of $U$.

### B. Method II: Constrained Optimization with Guaranteed Stability

In this method, we develop a data-driven constrained optimization framework for model reduction that also emphasizes stability of the reduced-order model. We introduce the approach through a sequence of developments.

*1) Weighted Least-squares Problem:* As a first step in the model-reduction method, consider the weighted least squares problem with cost function:

$$\begin{aligned} &J(A_{\rm r}, B_{\rm r}, C_{\rm r}, D_{\rm r}) \\ &= \left\| \left( \begin{bmatrix} \Delta_x^{k+1:k+l} \\ \Delta_y^{k:k+l-1} \end{bmatrix} - \begin{bmatrix} A_{\rm r} & B_{\rm r} \\ C_{\rm r} & D_{\rm r} \end{bmatrix} \begin{bmatrix} \Delta_x^{k:k+l-1} \\ \Delta_u^{k:k+l-1} \end{bmatrix} \right) R \right\|_{\rm F}, \end{aligned} \tag{12}$$

where $\|\cdot\|_{\rm F}$ denotes the Frobenius norm; $\Delta_x^{k+1:k+l}$, $\Delta_x^{k:k+l-1}$, $\Delta_y^{k:k+l-1}$, $\Delta_u^{k:k+l-1}$ are augmented data matrices for system state $x$, output, $y$, and input $u$ of the full-order model (of the same form in (9)); and $R$ is a weighting matrix. For subsequent developments, we will find it useful to express

$$J^2(A_{\rm r}, B_{\rm r}, C_{\rm r}, D_{\rm r}) = J_1^2(A_{\rm r}, B_{\rm r}) + J_2^2(C_{\rm r}, D_{\rm r}), \tag{13}$$

where

$$J_1 := \left\| \left( \Delta_x^{k+1:k+l} - [A_{\rm r}, B_{\rm r}] \begin{bmatrix} \Delta_x^{k:k+l-1} \\ \Delta_u^{k:k+l-1} \end{bmatrix} \right) R \right\|_{\rm F}, \tag{14}$$

$$J_2 := \left\| \left( \Delta_y^{k:k+l-1} - [C_{\rm r}, D_{\rm r}] \begin{bmatrix} \Delta_x^{k:k+l-1} \\ \Delta_u^{k:k+l-1} \end{bmatrix} \right) R \right\|_{\rm F}. \tag{15}$$

The optimal values of $C_{\rm r}, D_{\rm r}$, which we denote by $C_{\rm r}^\star, D_{\rm r}^\star$, respectively, can be obtained in closed-form quite straightforwardly from above. However, the solution to the above least squares problem will not necessarily yield a stable $A_{\rm r}$. In the following developments, we provide an approach to ensure stability.

*2) Guaranteeing Stability:* Asymptotic stability of $A_{\rm r}$ is equivalent to requiring the following Lyapunov inequality with a positive definite matrix $P$:

$$P - A_{\rm r} P A_{\rm r}^{\rm T} \succcurlyeq \delta I_{\rm r}. \tag{16}$$

We wish to ultimately reflect the above constraint in the weighted least-squares optimization problem. To do so, we first recognize using the Schur-complement lemma, that the

[1] We abuse notation slightly in the definition (9) with regard to (8) by denoting the states sampled from the full-order model also by $x_k$. Differences are indeed contextually evident.

above constraint can be equivalently expressed as:

$$\begin{bmatrix} P - \delta I_r & A_{\rm r} P \\ P A_{\rm r}^{\rm T} & P \end{bmatrix} \succcurlyeq 0, \tag{17}$$

where $\delta > 0$, and it is introduced to facilitate computation. Now consider expressing weighting matrix $R$ in the following form:

$$R = \begin{bmatrix} \Delta_x^{k:k+l-1} \\ \Delta_u^{k:k+l-1} \end{bmatrix}^{\ddagger} \begin{bmatrix} PR_1 & 0_{r\times m} \\ 0_{m\times r} & R_2 \end{bmatrix}, \tag{18}$$

where, $R_1 \in \mathbb{R}^{r\times r}$ and $R_2 \in \mathbb{R}^{m\times m}$, and with regard to notation,

$$V^{\ddagger} := V^{\rm T}(VV^{\rm T})^{\dagger},$$

with $(\cdot)^{\dagger}$ denoting the matrix pseudo-inverse. Substituting $R$ from (18) above in (12), we get the cost function:

$$\begin{aligned} &\widetilde{J}(A_{\rm r}, B_{\rm r}) \\ &= \left\| \left( \Delta_x^{k+1:k+l} \begin{bmatrix} \Delta_x^{k:k+l-1} \\ \Delta_u^{k:k+l-1} \end{bmatrix}^{\ddagger} \right. \\ &\left. \times \begin{bmatrix} PR_1 & 0_{r\times m} \\ 0_{m\times r} & R_2 \end{bmatrix} - \begin{bmatrix} A_{\rm r} P R_1 & B_{\rm r} R_2 \end{bmatrix} \right) \right\|_{\rm F}. \end{aligned} \tag{19}$$

We can express this in the form:

$$\widetilde{J}^2(A_{\rm r}, B_{\rm r}) = \widetilde{J}_1^2(A_{\rm r}) + \widetilde{J}_2^2(B_{\rm r}), \tag{20}$$

where

$$\widetilde{J}_1(A_{\rm r}) := \|(\Delta_1 - A_{\rm r}) P R_1\|_{\rm F}, \tag{21}$$

$$\widetilde{J}_2(B_{\rm r}) := \|(\Delta_2 - B_{\rm r}) R_2\|_{\rm F}, \tag{22}$$

$$\begin{bmatrix} \Delta_1 & \Delta_2 \end{bmatrix} := \Delta_x^{k+1:k+l} \begin{bmatrix} \Delta_x^{k:k+l-1} \\ \Delta_u^{k:k+l-1} \end{bmatrix}^{\ddagger}, \tag{23}$$

and $\Delta_1 \in \mathbb{R}^{n\times n}$ and $\Delta_2 \in \mathbb{R}^{n\times m}$. It is not hard to see that the minimizer for $B_{\rm r}$, $B_{\rm r}^{\star} = \Delta_2$.

Now, define the following change of variables

$$Q := A_{\rm r} P, \tag{24}$$

and consider the following semidefinite program,

$$\begin{aligned} \min_{P,Q} \quad & \|(\Delta_1 P - Q) R_1\|_{\rm F}^2 \\ \text{s.t.} \quad & \begin{bmatrix} P - \delta I_{\rm r} & Q \\ Q^{\rm T} & P \end{bmatrix} \succcurlyeq 0. \end{aligned} \tag{25}$$

With the optimal values of $P, Q$ denoted by $P^{\star}, Q^{\star}$, respectively, the optimal value of $A_{\rm r}^{\star}$ follows from (24) to be

$$A_{\rm r}^{\star} = Q^{\star}(P^{\star})^{-1}. \tag{26}$$

This is the method developed by Lacy and Bernstein [12] for system identification. The following section recasts (25) as a model reduction problem.

*3) Model Reduction:* The developments thus far enable identifying system matrices given data. We next describe how to extend this by introducing rank constraints in (25) to achieve a reduced-order system model. To be able to use solvers like CVX [17], we need a convex alternative to the rank of matrix $A_{\rm r}$. The following theorem [18] gives us a convex surrogate to the matrix rank.

**Theorem 1.** *The convex envelope of the function $\phi(X) = \operatorname{rank}(X)$ on $\mathcal{C} = \{X \in \mathbb{R}^{m\times n} \| \|X\| \leq 1\}$ is $\phi_{\rm env}(X) = \|X\|_*$, where $\|X\|_*$ is the nuclear norm of $X$.*

Thus, by penalizing $\|A_{\rm r}\|_*$, we can get a low-rank approximation of the system dynamics. However, $A_{\rm r}$ does not appear directly in (25), rather, it appears through $Q$. With that said, $\operatorname{rank}(Q) = \operatorname{rank}(A_{\rm r})$ because $P$ is full rank. Thus, we can reformulate (25) as:

$$\begin{aligned} \min_{P,Q} \quad & \|(\Delta_1 P - Q) R_1\|_{\rm F}^2 + \gamma \|Q\|_* \\ \text{s.t.} \quad & \begin{bmatrix} P - \delta I & Q \\ Q^{\rm T} & P \end{bmatrix} \succcurlyeq 0. \end{aligned} \tag{27}$$

This problem is convex, however, we observed that although the results obtained were accurate as well as of reduced order, the problem did not scale very well and is not very computationally efficient. In order to address this challenge, we use the following theorem [19], which allows us to obtain linear constraints corresponding to the positive semidefinite ones.

**Theorem 2.** *If a Hermitian matrix $X$ is diagonally dominant, i.e., $X_{ii} \geq \sum_{i\neq j} |X_{ij}|$ then $X \succcurlyeq 0$.*

Using Theorem 2, we modify (27) to get:

$$\begin{aligned} \min_{P,Q} \quad & \|(\Delta_1 P - Q) R_1\|_{\rm F}^2 + \gamma \|Q\|_* \\ \text{s.t.} \quad & P_{ii} \geq \sum_{i\neq j} |P_{ij}| + \sum_j |Q_{ij}| \\ & P_{ii} \geq \sum_{i\neq j} |P_{ij}| + \sum_j |Q_{ji}|. \end{aligned} \tag{28}$$

Replacing the positive semidefinite constraint in (15) with the linear constraints in (28) facilitates computations for larger problems.

## IV. Numerical Simulation Results

In this section, we present simulation results for Methods I and II introduced in Section III. Simulations are performed on a personal computer with an Intel Core i5 CPU and 16 GB RAM to reduce the model order of dynamics corresponding to a modified Kundur two-area power system discussed next. For the simulation setup, requisite data is collected by simulating the original nonlinear full-order model, although, conceivably, they could be collected from appropriate measurements.

### A. Modified Kundur Two-area System

The topology of the Kundur two-area system [20] used in the simulation studies is depicted in Fig. 1. It contains eleven buses with four generators connected to buses $1, 2, 3, 4$, and two $RLC$ loads, each connected to buses $7, 9$. The standard Kundur two-area model is modified by replacing the $PQ$ buses at $7, 9$ with parallel $RLC$ loads and by including a WECS with $N_{\rm tur} = 10$ at bus $4$. The full order model is described by a system dynamical model of order $n = 298$.

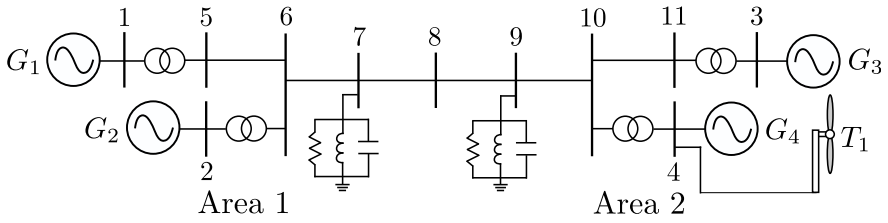


Fig. 1: Schematic depicting single-line diagram of a modified version of the Kundur two-area network used in the case studies. Buses 1 through 4 include synchronous generators $G_1$, $G_2$, $G_3$ and $G_4$. A WECS, denoted $T_1$ with $N_{\text{tur}} = 10$ turbines, is connected at bus 4. Impedance loads are connected at buses $7, 9$. The dimension of the state-space model corresponding to the original full-order model, $n = 298$.

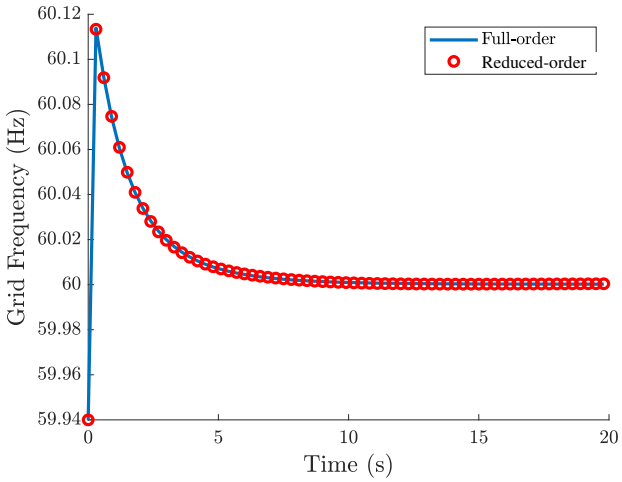


Fig. 2: Grid frequency at Bus #1 (See Fig. 1). Here, $r = 8$.

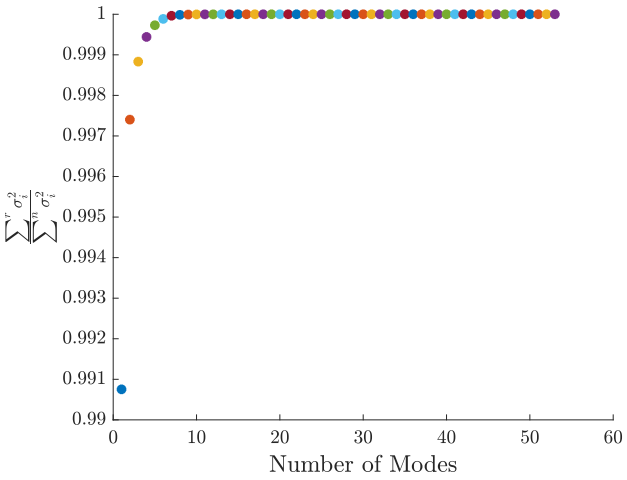


Fig. 3: Cumulative concentration of POD modes for $n = 53$. The curve saturates at $n = 8$ indicating that 8 modes are sufficient to capture the energy of the whole system.

The wind farm is first reduced using the aggregation technique described in [14]. This method relies on using parametric scalings to represent the dynamics of an entire wind farm as a single, large wind turbine. The resultant system is of state dimension 53. The results presented next apply the model reduction techniques described in Section III to this system to further reduce the state dimension.

### B. Results for Method I

In this section, we present some results that verify the accuracy of the POD-Galerkin approach. We first generate snapshots as in (9) from a simulation of the full-order model. (In practice, these data points could be collected from measurements.) Left singular vectors of this data gives us the principal directions of the system. Figure 2 compares the time-domain simulations of the grid frequency at Bus #1 of the reduced- and full-order models. These match up perfectly well. The number of columns of $U$ required to obtain $U_{\text{r}}$ is decided using inferences that can be drawn from Fig. 3 which plots the cumulative concentration of POD modes. It is clear from Fig. 3 that 8 columns of $U$ are sufficient to capture all the energy of the system. Thus, the resultant reduced-order model is order 8.

### C. Results for Method II

In this section, we focus on the convex-optimization-based method in Section III-B to obtain a reduced-order model description with stability guarantees. Figure 4 compares Bode plots of the full- and reduced-order models and demonstrates the accuracy of the reduced-order model. The reduced rank obtained by solving the optimization problem in (28) is 21. The matrix $A_{\text{r}}$ in the reduced-order model is of dimension 21, while the full-order matrix $A$ is of dimension 53. We note that (27) requires 75 sec of computation time, while with (28), we obtain the reduced-order model with 4 sec of computation time due to the linear constraint relaxation. Both of these computations are performed on CVX. The reduced system preserves stability and this can be seen from Fig. 5 which shows all the poles well within the unit circle.

## V. Concluding Remarks and Future Work

This paper describes two computational approaches for model reduction of power system dynamics. The first method is SVD-based and relies on an orthogonal projection of the dynamics on to a lower dimensional subspace while the second method relies on a convex-optimization based

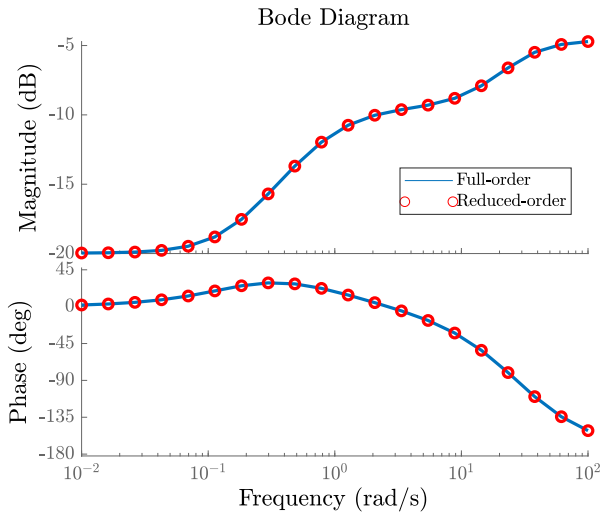


Fig. 4: Frequency response of the reduced and full-order systems.

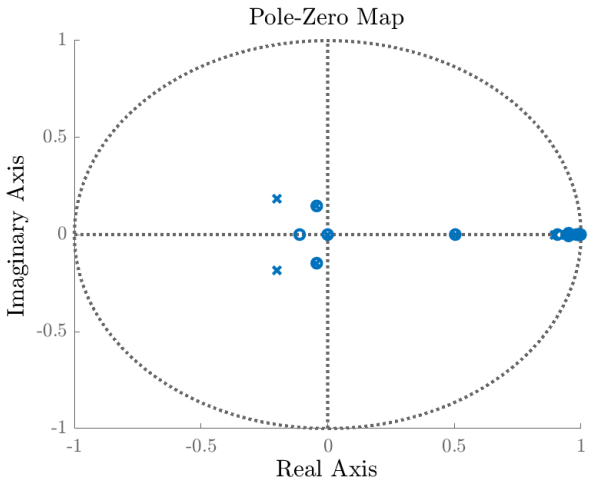


Fig. 5: Pole-zero map of the reduced system shows that the poles are well within the unit circle indicating that they are stable.

model-reduction method. While POD has computational advantages as computing the SVD is not very expensive, the optimization-based approach has guarantees on stability and gives us the freedom to add desirable constraints that can be utilized to impose structure and sparsity requirements. As part of future work, we will leverage the developed reduced-order models for stability analysis of low-inertia power networks with significant penetration of wind and solar resources.

## References


[1] S. Gugercin and A. C. Antoulas, "A survey of model reduction by balanced truncation and some new results," *International Journal of Control*, vol. 77, no. 8, pp. 748–766, 2004.

[2] M. G. Safonov and R. Chiang, "A Schur method for balanced-truncation model reduction," *IEEE Transactions on Automatic Control*, vol. 34, no. 7, pp. 729–733, 1989.

[3] B. Moore, "Principal component analysis in linear systems: Controllability, observability, and model reduction," *IEEE Transactions on Automatic Control*, vol. 26, no. 1, pp. 17–32, 1981.

[4] D. Chaniotis and M. Pai, "Model reduction in power systems using Krylov subspace methods," *IEEE Transactions on Power Systems*, vol. 20, no. 2, pp. 888–894, 2005.

[5] J. H. Chow, R. Galarza, P. Accari, and W. W. Price, "Inertial and slow coherency aggregation algorithms for power system dynamic model reduction," *IEEE Transactions on Power Systems*, vol. 10, no. 2, pp. 680–685, 1995.

[6] S. Gugercin, A. C. Antoulas, and C. Beattie, "$\mathcal{H}_2$ model reduction for large-scale linear dynamical systems," *SIAM Journal on Matrix Analysis and Applications*, vol. 30, no. 2, pp. 609–638, 2008.

[7] G. Xu and V. Vittal, "Slow coherency based cutset determination algorithm for large power systems," *IEEE Transactions on Power Systems*, vol. 25, no. 2, pp. 877–884, 2009.

[8] J. H. Chow, *Power system coherency and model reduction*. Springer, 2013.

[9] J. H. Chow, G. Peponides, P. Kokotovic, B. Avramovic, and J. Winkelman, *Time-scale modeling of dynamic networks with applications to power systems*, vol. 46. Springer, 1982.

[10] K. K. Anaparthi, B. Chaudhuri, N. F. Thornhill, and B. C. Pal, "Coherency identification in power systems through principal component analysis," *IEEE Transactions on Power Systems*, vol. 20, no. 3, pp. 1658–1660, 2005.

[11] A. T. Sari, M. T. Transtrum, and A. M. Stankovi, "Data-driven dynamic equivalents for power system areas from boundary measurements," *IEEE Transactions on Power Systems*, vol. 34, pp. 360–370, Jan 2019.

[12] S. L. Lacy and D. S. Bernstein, "Subspace identification with guaranteed stability using constrained optimization," *IEEE Transactions on Automatic control*, vol. 48, no. 7, pp. 1259–1263, 2003.

[13] P. W. Sauer and M. A. Pai, *Power system dynamics and stability*, vol. 101. Prentice hall Upper Saddle River, NJ, 1998.

[14] S. Vijayshankar, V. Purba, P. J. Seiler, and S. V. Dhople, "Reduced-order aggregate dynamical model for wind farms," in *2019 American Control Conference (ACC)*, pp. 5464–5471, July 2019.

[15] C. W. Rowley and S. T. Dawson, "Model reduction for flow analysis and control," *Annual Review of Fluid Mechanics*, vol. 49, pp. 387–417, 2017.

[16] K. Taira, S. L. Brunton, S. T. Dawson, C. W. Rowley, T. Colonius, B. J. McKeon, O. T. Schmidt, S. Gordeyev, V. Theofilis, and L. S. Ukeiley, "Modal analysis of fluid flows: An overview," *AIAA Journal*, pp. 4013–4041, 2017.

[17] M. Grant and S. Boyd, "CVX: Matlab software for disciplined convex programming, version 2.1." `http://cvxr.com/cvx`, Mar. 2014.

[18] B. Recht, M. Fazel, and P. A. Parrilo, "Guaranteed minimum-rank solutions of linear matrix equations via nuclear norm minimization," *SIAM review*, vol. 52, no. 3, pp. 471–501, 2010.

[19] G. H. Golub and C. F. Van Loan, *Matrix computations*, vol. 3. JHU press, 2012.

[20] P. Kundur, N. J. Balu, and M. G. Lauby, *Power system stability and control*, vol. 7. McGraw-hill New York, 1994.